Journal of Genetics and Genomics 44 (2017) 207–213

Contents lists available at ScienceDirect

Journal of Genetics and Genomics

Journal homepage: www.journals.elsevier.com/journal-of-genetics-and-genomics/

Method

A simple and efficient method for CRISPR/Cas9-induced mutant screening

Yufeng Hua [a, 1], Chun Wang [a, 1], Jian Huang [b, 1], Kejian Wang [a, *]

[a] State Key Laboratory of Rice Biology, China National Rice Research Institute, Chinese Academy of Agricultural Sciences, Hangzhou 310006, China
[b] School of Biology & Basic Medical Sciences, Soochow University, Suzhou 215123, China

ARTICLE INFO

Article history:
Received 9 January 2017
Received in revised form
17 February 2017
Accepted 7 March 2017
Available online 4 April 2017

Keywords:
ACT-PCR
CRISPR/Cas9
Genome editing
Mutant screening

ABSTRACT

The clustered regularly interspaced short palindromic repeats (CRISPR)/CRISPR-associated protein 9 (Cas9) system provides a technological breakthrough in mutant generation. Several methods such as the polymerase chain reaction (PCR)/restriction enzyme (RE) assay, T7 endonuclease I (T7EI) assay, Surveyor nuclease assay, PAGE-based genotyping assay, and high-resolution melting (HRM) analysis-based assay have been developed for screening CRISPR/Cas9-induced mutants. However, these methods are time- and labour-intensive and may also be sequence-limited or require very expensive equipment. Here, we described a cost-effective and sensitive screening technique based on conventional PCR, annealing at critical temperature PCR (ACT-PCR), for identifying mutants. ACT-PCR requires only a single PCR step followed by agarose gel electrophoresis. We demonstrated that ACT-PCR accurately distinguished CRISPR/Cas9-induced mutants from wild type in both rice and zebrafish. Moreover, the method can be adapted for accurately determining mutation frequency in cultured cells. The simplicity of ACT-PCR makes it particularly suitable for rapid, large-scale screening of CRISPR/Cas9-induced mutants in both plants and animals.

1. Introduction

Genetic mutants are critical for studying gene functions and analysing epistatic associations in genetic pathways. The recent development of sequence-specific nuclease systems such as transcription activator-like effector nucleases (TALENs), zinc finger nucleases (ZFNs), and particularly the type II clustered regularly interspaced short palindromic repeats (CRISPR)/CRISPR-associated protein 9 (Cas9) system has greatly expanded our ability to generate mutants at defined loci in many organisms (Li et al., 2013; Shan et al., 2013; Sander and Joung, 2014). The CRISPR-Cas9 system employs the CRISPR-associated endonuclease Cas9 and a single-guide RNA (sgRNA) to generate double-strand breaks (DSBs) at the target DNA site, subsequently leading to genetic mutations because of non-homologous end-joining (NHEJ) repair. Random insertion or deletion (indel) mutations induced by the CRISPR/Cas9 system usually occur proximate to the DSB site at 3 bp upstream of the protospacer-adjacent motif (PAM) (Cong et al., 2013). With the rapid popularity of genome editing in biological research, investigations regarding mutant isolation have significantly increased, particularly for large-scale screening.

To screen mutants produced by the CRISPR/Cas9 system, several approaches have been undertaken, such as the polymerase chain reaction (PCR)/restriction enzyme (RE) assay, T7 endonuclease I (T7EI) assay, Surveyor nuclease assay, PAGE-based genotyping assay, and high-resolution melting (HRM) analysis-based assay (Montgomery et al., 2007; Cong et al., 2013; Shan et al., 2014; Thomas et al., 2014; Zhu et al., 2014). However, each of these approaches has limitations such as being time- and labour-intensive, being sequence-limited, or requiring very expensive equipment. The PCR/RE assay is generally simple and sensitive for screening CRISPR/Cas9-induced mutants but is constrained by the availability of restriction enzyme sites near the target sequences. In contrast, the T7EI and Surveyor nuclease assays are wildly used and suitable for any target sequence as both can recognize and digest mismatched heteroduplex DNA; however, their detection sensitivity is lower than that of the PCR/RE assay, with both methodologies being time- and labour-intensive (Cong et al., 2013; Shan et al., 2014).

* Corresponding author.
E-mail address: wangkejian@caas.cn (K. Wang).
[1] These authors contributed equally to this work.

http://dx.doi.org/10.1016/j.jgg.2017.03.005

The PAGE-based genotyping assay, in which heteroduplex and homoduplex DNAs formed by brief denaturation and annealing of PCR-amplified genomic regions spanning the mutations are detected using native PAGE, remains time-consuming and is not high-throughput (Zhu et al., 2014). The HRM analysis-based approach based on the difference in melting temperature (T_m) between PCR amplicons with or without mutations can be successfully used for mutagenesis screening, but requires expensive equipment (Montgomery et al., 2007; Thomas et al., 2014). Several modified methods have also been developed for detecting CRISPR/Cas9-induced mutants that utilize microfluidic capillary electrophoresis or fluorescent PCR (Ramlee et al., 2015; Chenouard et al., 2016; Kc et al., 2016); however, these methods are expensive. A PCR-based method for detecting indel mutations in zebrafish has been recently reported (Yu et al., 2014), but it has limited sensitivity for detecting 1-bp indel mutations, which is the most common mutation type in CRISPR/Cas9-treated plants.

Here, we describe a simple, accurate, ultra-fast and inexpensive solution, annealing at critical temperature PCR (ACT-PCR), for detecting CRISPR/Cas9-induced mutations in both plants and animals. Moreover, by integration with real-time PCR, ACT-PCR can be used to accurately quantify mutation frequency in cultured cells.

2. Results

2.1. Schematic overview of ACT-PCR

PCR is a widely used technique that is capable of screening a large number of samples in a short time with high specificity. A single PCR cycle comprises three steps: denaturation, annealing and extension. The annealing temperature is critical for primer-template pairing for the success of PCR. An optimal temperature suppresses mismatched annealing, thereby reducing the generation of non-specific products. On the basis of this theory, we developed ACT-PCR to detect CRISPR/Cas9-induced mutants easily, accurately, rapidly and inexpensively. This method comprises three steps: 1) design of primers, 2) detection of the critical annealing temperature by preliminary gradient PCR, and 3) screening of mutants. First, primer pairs specific for target genes were designed. The forward primer, named the DSB site-specific (DS) primer, flanks the DSB site with its 3′ end containing a 1–4-bp overhang relative to the DSB site to ensure specificity and sensitivity for wild-type (WT) gene binding and PCR amplification; the reverse primer is located outside the DSB site and has a higher T_m value than the DS primer to ensure DNA template binding at the critical annealing temperature. Next, preliminary gradient PCR was performed to determine the critical annealing temperature. Finally, conventional PCR was performed at the determined critical annealing temperature. If a mutation is present, the DS primer will not bind to the mutated sequence and no amplicons will be obtained (Fig. 1). Thus, mutants are identified on the basis of the absence of WT amplicons.

2.2. Identification of CRISPR/Cas9-induced mutants in rice

We previously developed a simple and efficient CRISPR/Cas9 multiplex genome editing system to simultaneously mutate phytoene desaturase (*OsPDS*), *Os02g23823* and *OsMPK2* genes in rice, and obtained 110 T_0 transgenic plants in which the mutation types of all these three targets were identified by the PCR/RE assay and/or sequencing (Wang et al., 2015). In this study, we selected 22 of these T_0 plants (lines #1–22) to test the accuracy of ACT-PCR. We first detected *Ospds* mutants in these T_0 plants. Four 20-bp DS primers with a 1-bp (*PDS*-DS1), 2-bp (*PDS*-DS2), 3-bp (*PDS*-DS3), or 4-bp (*PDS*-DS4) overhang relative to the DSB site were designed along with a common reverse primer (*PDS*-R) (Fig. 2A). A preliminary gradient PCR was then performed at annealing temperatures that ranged from 55°C to 72°C using WT genomic DNA as the templates to determine the critical annealing temperature of each primer pair (*PDS*-DS1/*PDS*-R: 66.7°C; *PDS*-DS2/*PSD*-R: 64.8°C; *PDS*-DS3/*PSD*-R: 66.7°C; *PDS*-DS4/*PSD*-R: 66.7°C) (Fig. 2A). We then screened the 22 T_0 plants by PCR amplification using these four primer pairs under their corresponding critical annealing temperatures (Fig. 2B). All pairs, except *PDS*-DS1/*PDS*-R, correctly identified the *Ospds* mutants. We previously revealed a 1-bp cytosine (C) insertion at the DSB site in one allele of lines #7 and #13 (Wang et al., 2015). The *PDS*-DS1 primer could still match the mutated sequence, and those two lines were accidentally judged. In theory, the error frequency is negatively related to the number of nucleotide overhangs (n) in the forward primer relative to the DSB site (4^{-n}). Therefore, we designed forward primers containing 4-bp overhangs relative to the DSB sites in the following experiments.

To verify the accuracy of ACT-PCR for identifying multiplexed genome-modified plants, we designed *Os02g23823*-DS and *Os02g23823*-R primers to detect *Os02g23823* mutants in the 22 T_0 plants (Wang et al., 2015). The critical annealing temperature was determined to be 63.0°C (Fig. S1). In the subsequent PCR, amplifications were disrupted in the *Os02g23823* mutants (Fig. 2B). Combined with the ACT-PCR detection results for *Ospds* described above, lines #1, #2, #3, #7, #8, #10, #11, #12, #13 and #16 were identified as double mutants (*Ospds*/*Os02g23823*), consistent with our previously reported results and suggesting that ACT-PCR can be used for accurately and rapidly identifying multiplexed genome-modified mutants. In addition, all mutants were identified regardless of the mutation types, indicating that ACT-PCR can be used for screening different mutation types introduced by CRISPR/Cas9.

Recently, using the CRISPR/Cas9 multiplex genome editing system (Wang et al., 2015), we also designed a vector to simultaneously target eight rice agronomic genes, including *Betaine Aldehyde Dehydrogenase 2* (*BADH2*), *dense and erect panicle 1* (*DEP1*), *grain number* (*Gn1a*), *major quantitative trait loci (QTL) for grain length and weight* (*GS3*), *major QTL associated with rice grain width and weight* (*GW2*), *Heading date 1* (*Hd1*), *ERECT PANICLE* (*EP3*), and *Loose Plant Architecture1* (*LPA1*), and obtained 36 T_0 transgenic plants whose genotypes have been identified by direct DNA sequencing (Shen et al., 2017). To further test the accuracy of ACT-PCR in multiplex mutant identification, we detected all mutation sites of the 36 T_0 plants by ACT-PCR. The critical annealing temperatures of *DEP1*, *GW2*, *EP3* and *GS3* targets were determined to be 64.8°C, 63.0°C, 64.8°C and 64.8°C, respectively, using *Taq* DNA polymerase (Fig. S2A). The critical annealing temperatures of *BADH2*, *Gn1a* and *LPA1* targets were determined to be 63.8°C, 65.4°C and 65.4°C, respectively, using KOD FX DNA polymerase, because no products could be amplified by *Taq* DNA polymerase (Fig. S2A). However, we failed to determine the critical annealing temperature of *Hd1* target because no amplicons could be obtained using *Taq* DNA polymerase or KOD FX DNA polymerase. The results showed that the genotypes of the seven target genes in 36 T_0 plants detected by ACT-PCR were consistent with those identified by direct DNA sequencing (Fig. S2B). These results, especially the identification of the hepta-mutants lines #19 and #35 (Fig. S2B), further verify the accuracy of ACT-PCR in multiplex mutant identification.

In cases the CRISPR/Cas9-induced mutation frequency is low in T_0 transgenic plants, isolation of homozygous mutants from the T_1 generation of heterozygous T_0 plants may be required. We

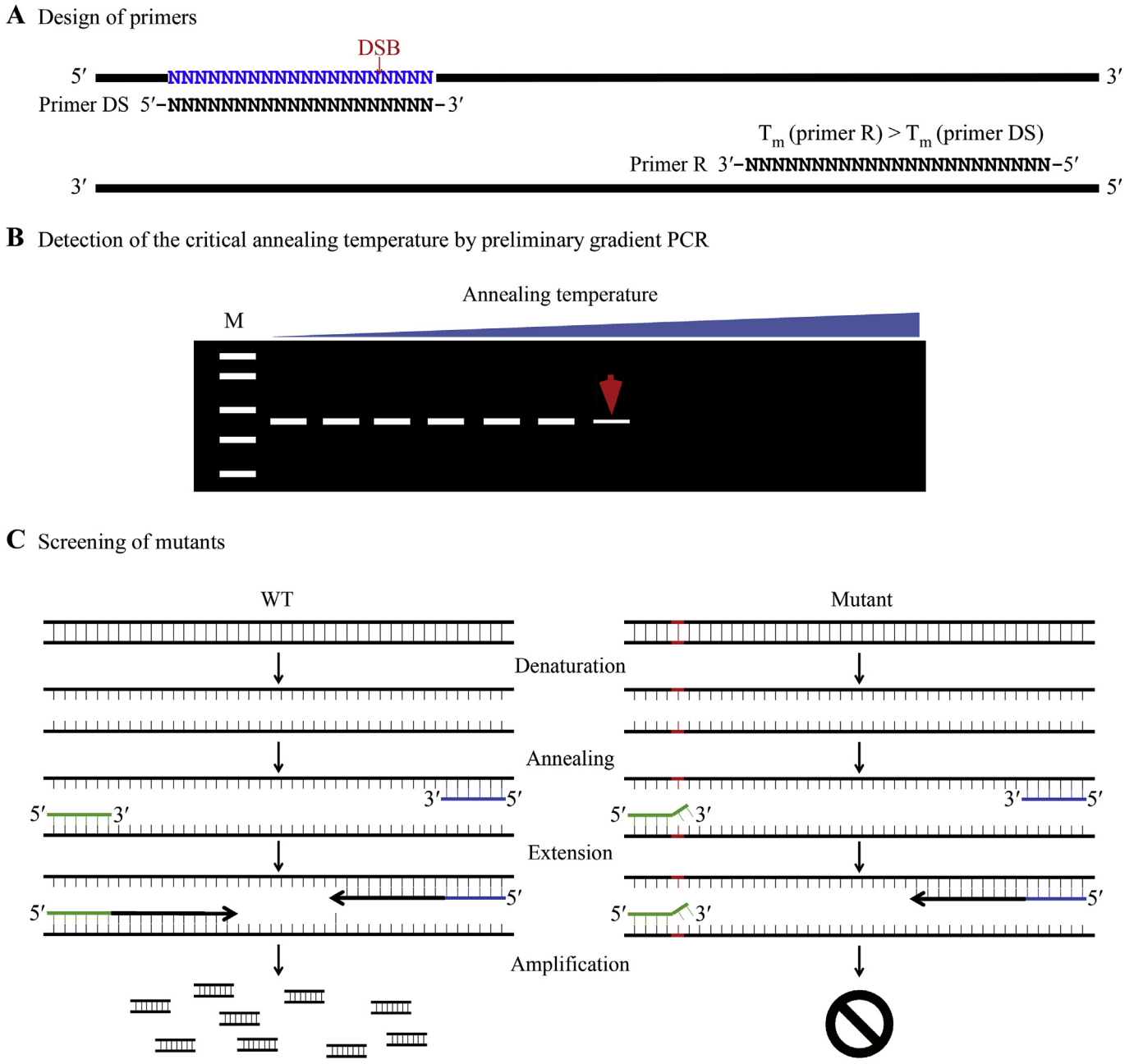

Fig. 1. Schematic illustration of ACT-PCR. **A**: Design of primers. The forward primer, double-strand break site-specific (DS) primer, is designed with a 1–4-bp overhang relative to the DSB site. The reverse primer, primer R, is designed with a higher melting temperature (T_m) value than the DS primer. **B**: Detection of the critical annealing temperature by preliminary gradient PCR. The critical annealing temperature (red arrow) is defined as the highest temperature at which PCR products could be detected. **C**: Screening of mutants. The primer DS, primer R and mutation site are labelled in green, blue and red, respectively. At the critical annealing temperature, amplicons could be obtained from the wild-type (WT) gene but not from the CRISPR/Cas9-induced mutant because of the introduction of mismatches at the target site.

previously successfully generated heterozygous plants of liguleless gene *OsLG1* and *Glossy1*-homologous gene *OsGL1-1* using the Cas9 VQR variant which recognises the NGA PAMs (Hu et al., 2016). Here, we selected the T_1 generation of these plants to screen for homozygous mutants using ACT-PCR. The critical annealing temperatures of both *OsLG1* and *OsGL1-1* primers were found to be 66.7°C (Fig. 3A and B). Subsequent PCR showed that amplifications were disrupted in 5 of the 24 *OsLG1* T_1 plants and 7 of the 36 *OsGL1-1* T_1 plants (Fig. 3C and D). PCR/RE assay and direct DNA sequencing further confirmed that all T_1 plants that displayed disrupted amplifications were homozygous mutants (Figs. 3C, 3D and S3), indicating that ACT-PCR can also be used for mutant screening in later generations.

2.3. Identification of CRISPR/Cas9-induced mutants in zebrafish

To test the efficiency of ACT-PCR screening in animals, we generated zebrafish mutants using the CRISPR/Cas9 system. The *lphn3.1* (ENSDARG00000061121), *glycogenin2* (ENSDARG00000033380) and *per3* (ENSDARG00000010519) genes were coedited by a single microinjection of *Cas9* RNA plus gene-specific sgRNAs into zebrafish one-cell embryos. Specific DS and reverse primers were designed (Table S1), and then the critical

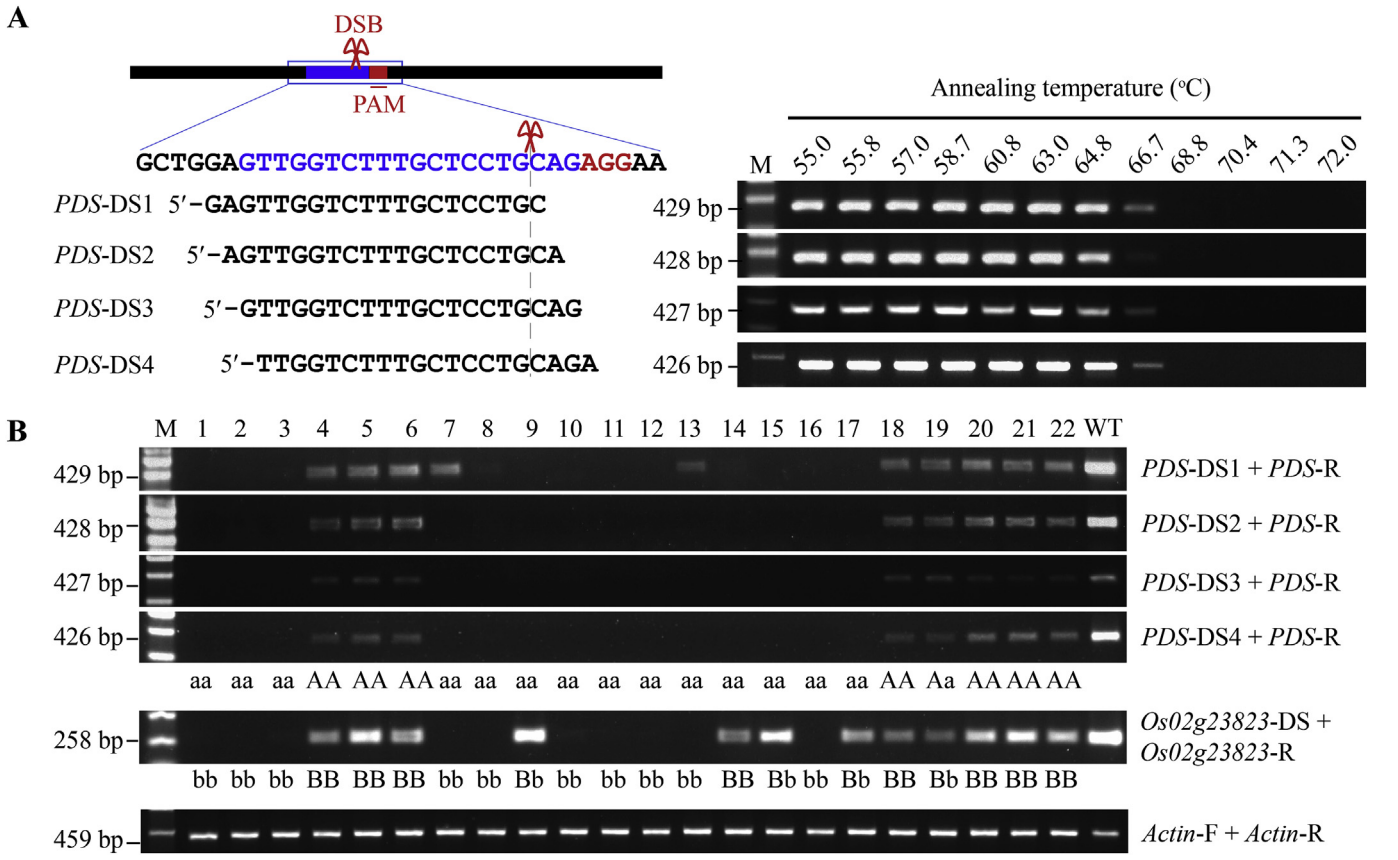

Fig. 2. Identification of the CRISPR/Cas9-induced mutants in rice using ACT-PCR. **A**: The critical annealing temperatures detected by preliminary gradient PCR using four primer pairs designed for the *OsPDS* target. The wild-type (WT) sequence of *OsPDS* is shown at the top. The target sequences are labelled in blue, and the PAM is labelled in red. The DSB site is indicated with a scissor. The sequences of the *PDS*-DS1, *PDS*-DS2, *PDS*-DS3 and *PDS*-DS4 primers are listed under the WT sequence. **B**: ACT-PCR analysis of *Ospds* and *Os02g23823* mutants in the T_0 transgenic rice plants. In the bottom gel, *OsActin* was amplified as the control. The genotypes identified by DNA sequencing are listed under the gels. 'A' and 'a' indicate the functional and non-functional alleles at the *OsPDS* locus, respectively; 'B' and 'b' indicate the functional and non-functional alleles at the *Os02g23823* locus, respectively.

annealing temperatures were determined by gradient PCR from 55°C to 72°C using WT zebrafish genomic DNA as the template. The critical annealing temperatures of *lphn3.1*, *glycogenin2* and *per3* targets were 66.7°C, 64.8°C and 68.8°C, respectively (Fig. 4A). Using ACT-PCR, line #2 was identified as a *lphn3.1* mutant, #3 as a *glycogenin2* mutant, and #4 and #5 as *per3* mutants (Fig. 4B). All mutants were further confirmed using DNA sequencing (Fig. S4). These results suggest that ACT-PCR is an appropriate method for mutant screening in both animals and plants.

2.4. Expanding ACT-PCR for accurately quantifying mutation frequency

For many experimental applications, particularly those using cultured cells, accurate quantification of mutation frequency is required. To test whether ACT-PCR can be adapted for accurately quantifying the mutation frequency, we created an *in vitro* model of mutation frequency variation by mixing several *Ospds* mutant DNA sequences with WT DNA in ratios from 0 to 1 (no mutant to 100% mutant). As 1-bp indel is the main mutation type induced by CRISPR/Cas9 in rice, mutant DNA containing only a 1-bp insertion was selected for the quantitative ACT-PCR (Fig. 5A). For comparison, the PCR/RE and T7EI assays were also conducted as previously described (Shan et al., 2014). Mutation ratios calculated by quantitative ACT-PCR were consistent with the actual values, whereas those estimated by the PCR/RE assay were significantly deviated from the actual values, suggesting that the PCR/RE assay is useful only for approximately estimating mutation efficiency (Fig. 5A and B). Unexpectedly, the T7EI assay did not generate clear bands for mutation efficiency estimation (Fig. 5C), suggesting that the T7EI assay does not efficiently detect 1-bp indels (the most frequently induced mutations in plants). We then conducted CRISPR/Cas9-mediated genome editing in rice protoplasts and quantified mutation frequency using both quantitative ACT-PCR and PCR/RE assays (Fig. 5D). Both experiments showed that the mutation ratio of *OsPDS* target was approximately 20%. The results implied that ACT-PCR can be used for quantitatively estimating the editing efficiency in cultured cells.

3. Discussion

In this study, we developed ACT-PCR to identify CRISPR/Cas9-induced mutants. In contrast to other methods for mutant identification, ACT-PCR requires only conventional PCR and agarose gel electrophoresis (Table 1). Moreover, ACT-PCR is highly sensitive for identifying CRISPR/Cas9-induced mutants, even 1-bp indels. Compared with the PCR/RE assay, ACT-PCR can be utilized for detection regardless of available restriction enzyme sites. Moreover, unlike HRM analysis, ACT-PCR does not require expensive equipment. Notably, while the method was developed for mutant screening, quantitative ACT-PCR could also be performed for heterozygote screening, and other methods such as PCR/RE and T7EI

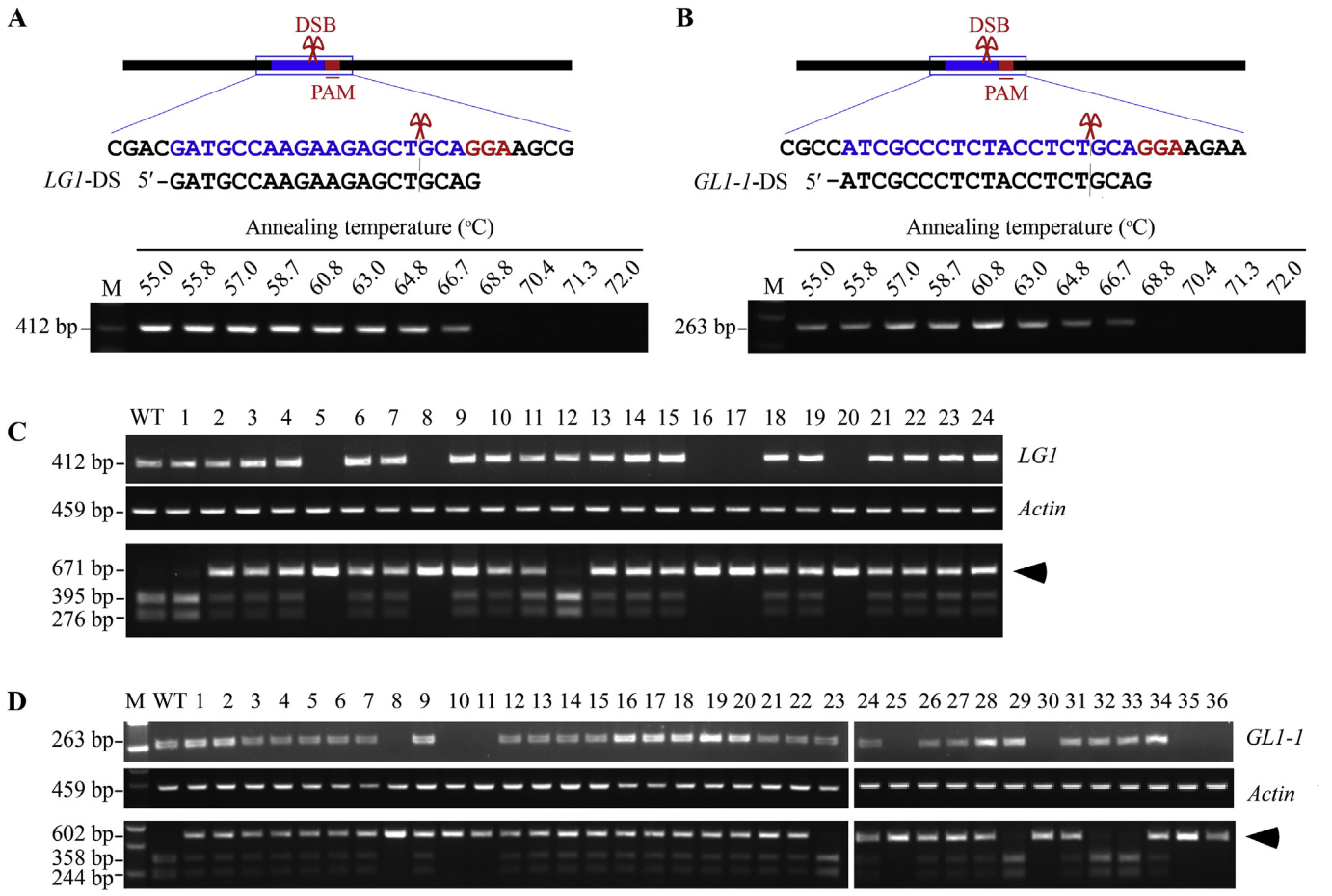

Fig. 3. Isolation of homozygous mutants from the T_1 generation of heterozygous T_0 plants using ACT-PCR. **A** and **B**: The critical annealing temperatures detected by gradient PCR using specific primers for the *OsLG1* target (**A**) and the *OsGL1-1* target (**B**), respectively. **C**: ACT-PCR analysis of *Oslg1* mutants in the T_1 generation of transgenic rice plants. *OsActin* was amplified as the control. In the bottom gel, the mutations at proximate *OsLG1* target sites were detected by PCR/RE assay with *Pst* I digestion. Black arrowhead indicates the bands used for identifying mutations. Lines #5, #8, #16, #17 and #20 are homozygous mutants detected by both ACT-PCR and PCR/RE assays. **D**: ACT-PCR analysis of *Osgl1-1* mutants in the T_1 generation of transgenic rice plants. *OsActin* was amplified as the control. In the bottom gel, the mutations at proximate *OsGL1-1* target sites were detected by PCR/RE assay with *Pst* I digestion. Black arrowhead indicates the bands used for identifying mutations. Lines #8, #10, #11, #25, #30, #35 and #36 are homozygous mutants detected by both ACT-PCR and PCR/RE assays.

assays can also be used as complementary strategies to isolate heterozygotes.

A previous report also described a PCR-based assay for detecting indel mutations and mutation frequency in zebrafish, in which the primers used had only a 1-bp overlap with the DSB site (Yu et al., 2014). Genome editing in zebrafish performed by direct microinjection tends to introduce large deletions in the genome (>2 bp); therefore, in most cases, the primer will be mismatched with the mutated DNA. In contrast to zebrafish, the most frequent mutation type in plants is the 1-bp indel. According to our results, detection using primers with 1-bp overhangs (DS1) relative to the DSB site will markedly increase the error frequency (approximately 25%) in detecting 1-bp indels, thereby limiting the applicability of such primers in plants. In the present study, we found that primers with 4-bp overhangs (DS4) relative to the DSB site will efficiently reduce the error frequency, and PCR performed at the critical annealing temperature will effectively inhibit the generation of non-specific products. These modifications substantially enhanced the detection of 1-bp indels in both plants and animals.

In summary, the simplicity of ACT-PCR makes it particularly suitable for the rapid screening of CRISPR/Cas9 mutants in both plants and animals.

4. Materials and methods

4.1. Plant materials

The process of generating mutants by the CRISPR/Cas9 system (Cas9 and Cas9 VQR variant) has been described in previous studies (Wang et al., 2015; Hu et al., 2016). Genomic DNA was extracted from rice using the cetyltrimethyl ammonium bromide (CTAB) method.

4.2. Zebrafish maintenance and embryo production

The zebrafish WT AB strain was grown in a 14-h/10-h light/dark cycle at 28°C. Embryos were produced by pair mating and maintained in culture dishes. One-cell-stage embryos were used for Cas9/sgRNA microinjection.

4.3. Preparation of Cas9 RNA and sgRNAs and mutagenesis screening in zebrafish

Cas9 RNA and gene-specific sgRNAs were prepared as previously described (Irion et al., 2014), and then co-microinjected in pair into

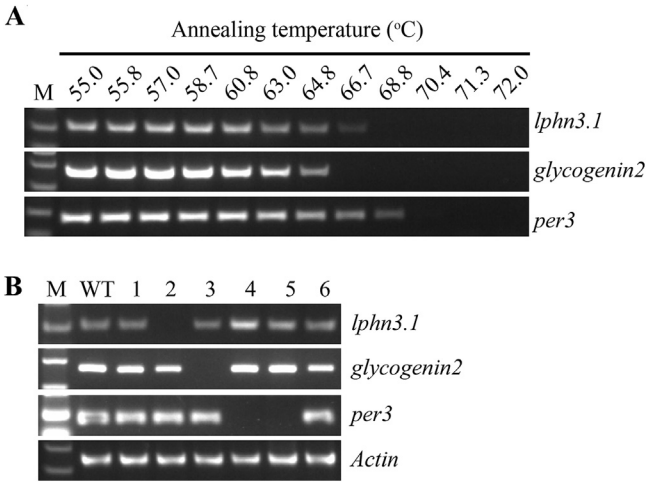

Fig. 4. Identification of the CRISPR/Cas9-induced mutants in zebrafish using ACT-PCR. **A**: The critical annealing temperatures detected by gradient PCR using specific primers for the *lphn3.1*, *glycogenin2* and *per3* targets, respectively. **B**: ACT-PCR analysis of *lphn3.1*, *glycogenin2* and *per3* mutants. In the bottom gel, the zebrafish *Actin* gene was amplified as the control.

one-cell zebrafish embryos at a concentration of 250 pg. The microinjected embryos were maintained in E3 medium (5 mM NaCl, 0.17 mM KCl, 0.33 mM $CaCl_2$, 0.33 mM $MgSO_4$) at 28.5°C. Genomic DNA was extracted from approximate 10 embryos at 2 days post-fertilisation.

4.4. PCR

When using *Taq* DNA polymerase to amplify PCR products, the amplification was performed with 50 ng genomic DNA in a 15-μL reaction volume containing 0.3 μM of each specific forward and reverse primer, and 2× *Taq* Master Mix (Novoprotein Scientific, China). The thermocycler was set at 94°C for 3 min, 33 cycles at 94°C for 30 s, 12 gradient annealing temperatures (from 55°C to 72°C) for 30 s for gradient PCR or critical annealing temperature for 30 s for ACT-PCR, and 72°C for 30 s, followed by 72°C for 2 min and 18°C for 2 min.

When using KOD FX DNA polymerase to amplify PCR products, the amplification was carried out in a 15-μL reaction volume containing 7.5 μL of 2× PCR buffer for KOD FX DNA polymerase, 3 μL of 2 mM dNTPs, 0.3 μL of KOD FX (1.0 U/μL, Toyobo, Japan), 50 ng of genomic DNA and 0.3 μM of each specific forward and reverse primer. The thermocycler was set at 94°C for 2 min, then 33 cycles at 98°C for 10 s, 12 gradient annealing temperatures (from 55°C to 68°C) for 30 s for gradient PCR or critical annealing temperature for 30 s for ACT-PCR, and 68°C for 30 s, followed by 68°C for 5 min and 18°C for 2 min.

The PCR products were detected using 1.5% agarose gels. The critical annealing temperature was defined as the highest temperature at which PCR products could be detected. The PCR primers used are listed in Table S1.

4.5. Detection of mutations using PCR/RE and DNA sequencing

PCR was performed to amplify the genomic regions surrounding the CRISPR/Cas9 target site(s). The PCR fragments were then digested with *Pst* I. PCR products were further sequenced, and multiple peaks were decoded by the Degenerate Sequence

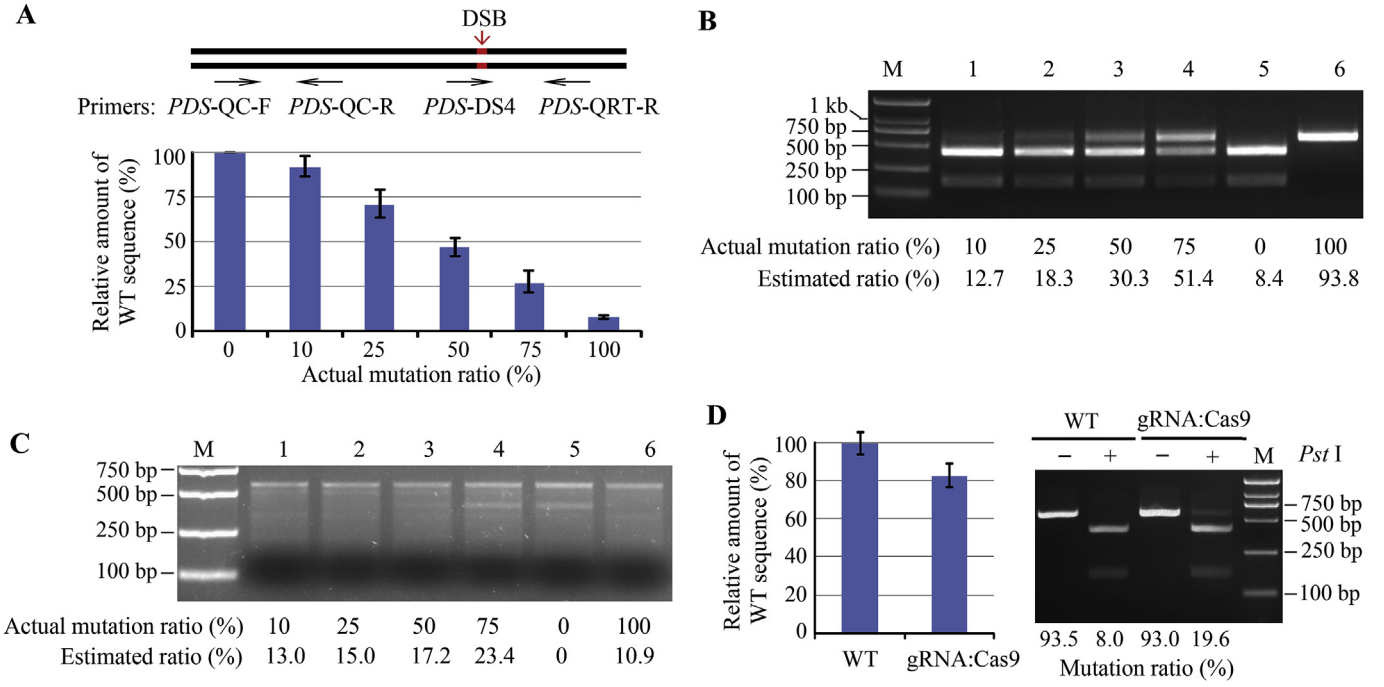

Fig. 5. Adapting ACT-PCR for accurately quantifying mutation frequency. **A**: Determination of mutation ratio using quantitative ACT-PCR. Different ratios of mutant *Ospds* DNA (harbouring a 1-bp insertion) and wild-type (WT) DNA were prepared. *PDS*-DS4 and *PDS*-QRT-R primers were used for ACT-PCR. The *PDS*-QC-F and *PDS*-QC-R primers were applied as an endogenous control. **B**: Determining mutation ratio using the PCR/RE assay. The PCR products were digested with *Pst* I. **C**: Determining mutation ratio using the T7EI assay. **D**: Quantifying mutation frequency of genome-edited rice protoplasts by quantitative ACT-PCR (left) and the PCR/RE assay (right). WT, protoplasts without editing; gRNA:Cas9, protoplasts with editing at the *OsPDS* locus. Data are represented as mean ± SD of three technical repeats.

Table 1
Comparison of ACT-PCR with other methods for CRISPR/Cas9-induced mutant screening.

Approach	Time (h)	Accuracy	Labour	Cost	Applicable sequence
ACT-PCR method	1–2	High	Low	Low	No limit
T7EI assay	>4	Moderate	Moderate	Moderate	No limit
PCR/RE assay	>4	High	Moderate	Moderate	Limited
PAGE-based method	>4	Moderate	High	Moderate	No limit
HRM analysis	2–3	Moderate	Moderate	High	No limit

Decoding (DSD) method to confirm mutations in the rice genome (Ma et al., 2015).

4.6. Gene editing in rice protoplasts and quantitative analysis of mutation efficiency by quantitative ACT-PCR

Rice protoplast transformation was performed as previously described (Shan et al., 2014). The plasmids pJIT163-2NLSCas9 and sgRNA-PDS were co-transfected into rice protoplasts using the polyethylene glycol mediated method. After transfection, protoplasts were cultured in the dark at 28°C for 48 h. Protoplast genomic DNA was extracted using the CTAB method.

To optimize quantitative ACT-PCR, we designed a new reverse primer (named *PDS*-QRT-R) to meet the real-time PCR criteria. PCR was performed in a 20-μL reaction volume containing 50 ng of genomic DNA, 0.4 μM of *PDS*-DS4 and *PDS*-QRT-R, and 2× qPCR SYBR Green Master Mix. Reactions were run using the CFX96™. Real-time System with thermocycling conditions of 95°C for 5 min, then 40 cycles at 95°C for 10 s, critical annealing temperature for 20 s and 72°C for 30 s, followed by a gradient from 60°C to 95°C with continuous detection at 0.1°C/s. Relative amounts of target PCR products were normalised to the endogenous control PCR product amplified by primers of *PDS*-QC-F and *PDS*-QC-R, and analyzed using the ΔCt method. Each sample was processed in triplicate.

4.7. Estimation of the indel frequency by the PCR/RE and T7EI assays

To estimate indel frequency by the PCR/RE assay, the intensities of undigested PCR amplicons and digested bands were measured as previously described (Shan et al., 2014) using ImageJ (NIH). Indel (%) was then calculated according to the following formula003A

$$\text{indel}(\%) = 100 \times \frac{a}{(a+b+c)}$$

where a is the intensity of the undigested PCR products, and b and c are the intensities of two digested products.

To estimate indel frequency by the T7EI assay, the intensities of the undigested PCR amplicons and digested bands were measured using ImageJ (NIH). Indel (%) was then calculated according to the following formula:

$$\text{indel}(\%) = 100 \times \left(1 - \sqrt{1 - \frac{b+c}{a+b+c}}\right)$$

where a is the intensity of undigested PCR products, and b and c are the intensities of the two digested products.

Acknowledgments

We thank Prof. Jixian Zhai (Southern University of Science and Technology, China) for critical reviewing the manuscript. This study was supported by the National Natural Science Foundation of China (Nos. 31271681 and 3140101312) and the Agricultural Science and Technology Innovation Program of Chinese Academy of Agricultural Sciences.

Supplementary data

Supplementary data related to this article can be found at http://dx.doi.org/10.1016/j.jgg.2017.03.005.

References

Chenouard, V., Brusselle, L., Heslan, J.M., Remy, S., Menoret, S., Usal, C., Ouisse, L.H., TH, N.G., Anegon, I., Tesson, L., 2016. A rapid and cost-effective method for genotyping genome-edited animals: a heteroduplex mobility assay using microfluidic capillary electrophoresis. J. Genet. Genomics 43, 341–348.
Cong, L., Ran, F.A., Cox, D., Lin, S., Barretto, R., Habib, N., Hsu, P.D., Wu, X., Jiang, W., Marraffini, L.A., Zhang, F., 2013. Multiplex genome engineering using CRISPR/Cas systems. Science 339, 819–823.
Hu, X., Wang, C., Fu, Y., Liu, Q., Jiao, X., Wang, K., 2016. Expanding the range of CRISPR/Cas9 genome editing in rice. Mol. Plant 9, 943–945.
Irion, U., Krauss, J., Nusslein-Volhard, C., 2014. Precise and efficient genome editing in zebrafish using the CRISPR/Cas9 system. Development 141, 4827–4830.
Kc, R., Srivastava, A., Wilkowski, J.M., Richter, C.E., Shavit, J.A., Burke, D.T., Bielas, S.L., 2016. Detection of nucleotide-specific CRISPR/Cas9 modified alleles using multiplex ligation detection. Sci. Rep. 6, 32048.
Li, J.F., Norville, J.E., Aach, J., McCormack, M., Zhang, D., Bush, J., Church, G.M., Sheen, J., 2013. Multiplex and homologous recombination-mediated genome editing in *Arabidopsis* and *Nicotiana benthamiana* using guide RNA and Cas9. Nat. Biotechnol. 31, 688–691.
Ma, X., Chen, L., Zhu, Q., Chen, Y., Liu, Y.G., 2015. Rapid decoding of sequence-specific nuclease-induced heterozygous and biallelic mutations by direct sequencing of PCR products. Mol. Plant 8, 1285–1287.
Montgomery, J., Wittwer, C.T., Palais, R., Zhou, L., 2007. Simultaneous mutation scanning and genotyping by high-resolution DNA melting analysis. Nat. Protoc. 2, 59–66.
Ramlee, M.K., Yan, T., Cheung, A.M., Chuah, C.T., Li, S., 2015. High-throughput genotyping of CRISPR/Cas9-mediated mutants using fluorescent PCR-capillary gel electrophoresis. Sci. Rep. 5, 15587.
Sander, J.D., Joung, J.K., 2014. CRISPR-Cas systems for editing, regulating and targeting genomes. Nat. Biotechnol. 32, 347–355.
Shan, Q., Wang, Y., Li, J., Gao, C., 2014. Genome editing in rice and wheat using the CRISPR/Cas system. Nat. Protoc. 9, 2395–2410.
Shan, Q., Wang, Y., Li, J., Zhang, Y., Chen, K., Liang, Z., Zhang, K., Liu, J., Xi, J.J., Qiu, J.L., Gao, C., 2013. Targeted genome modification of crop plants using a CRISPR-Cas system. Nat. Biotechnol. 31, 686–688.
Shen, L., Hua, Y., Fu, Y., Li, J., Liu, Q., Jiao, X., Xin, G., Wang, J., Wang, X., Yan, C., Wang, K., 2017. Rapid generation of geneitc diversity by multiplex CRISPR/Cas9 genome editing in rice. Sci. China Life Sci. http://dx.doi.org/10.1007/s11427-017-9008-8.
Thomas, H.R., Percival, S.M., Yoder, B.K., Parant, J.M., 2014. High-throughput genome editing and phenotyping facilitated by high resolution melting curve analysis. PLoS One 9, e114632.
Wang, C., Shen, L., Fu, Y., Yan, C., Wang, K., 2015. A simple CRISPR/Cas9 system for multiplex genome editing in rice. J. Genet. Genomics 42, 703–706.
Yu, C., Zhang, Y., Yao, S., Wei, Y., 2014. A PCR based protocol for detecting indel mutations induced by TALENs and CRISPR/Cas9 in zebrafish. PLoS One 9, e98282.
Zhu, X., Xu, Y., Yu, S., Lu, L., Ding, M., Cheng, J., Song, G., Gao, X., Yao, L., Fan, D., Meng, S., Zhang, X., Hu, S., Tian, Y., 2014. An efficient genotyping method for genome-modified animals and human cells generated with CRISPR/Cas9 system. Sci. Rep. 4, 6420.